The Astrophysical Journal, 756:83 (6pp), 2012 September 1 doi:10.1088/0004-637X/756/1/83

A UNIFYING PICTURE OF HELICAL AND AZIMUTHAL MAGNETOROTATIONAL INSTABILITY, AND THE UNIVERSAL SIGNIFICANCE OF THE LIU LIMIT

Oleg N. Kirillov[1], Frank Stefani[1], and Yasuhide Fukumoto[2]
[1] Helmholtz-Zentrum Dresden-Rossendorf, P.O. Box 510119, D-01314 Dresden, Germany; o.kirillov@hzdr.de, f.stefani@hzdr.de
[2] Institute of Mathematics for Industry, Kyushu University, 744 Motooka, Nishi-ku, Fukuoka 819-0395, Japan; yasuhide@imi.kyushu-u.ac.jp
Received 2012 May 4; accepted 2012 June 25; published 2012 August 20

ABSTRACT

The magnetorotational instability (MRI) plays a key role for cosmic structure formation by triggering turbulence in the rotating flows of accretion disks that would be otherwise hydrodynamically stable. In the limit of small magnetic Prandtl number, the helical and the azimuthal versions of MRI are known to be governed by a quite different scaling behavior than the standard MRI with a vertical applied magnetic field. Using the short-wavelength approximation for an incompressible, resistive, and viscous rotating fluid, we present a unified description of helical and azimuthal MRI, and we identify the universal character of the Liu limit $2(1-\sqrt{2}) \approx -0.8284$ for the critical Rossby number. From this universal behavior we are also led to the prediction that the instability will be governed by a mode with an azimuthal wavenumber that is proportional to the ratio of axial to azimuthal applied magnetic field, when this ratio becomes large and the Rossby number is close to the Liu limit.

Key words: instabilities – magnetohydrodynamics (MHD) – waves

Online-only material: color figures

1. INTRODUCTION

The magnetorotational instability (MRI) is widely accepted as the main source of turbulence and outward angular momentum transport that is needed for the matter in accretion disks to spiral inward onto the central protostar or black hole (Balbus & Hawley 1991). While the early work on MRI was mainly concerned with ideal magnetohydrodynamics, the last years have seen an increasing interest in the influence of viscosity and electrical resistivity on the MRI (Pessah & Chan 2008). A particular role is thought to be played by the magnetic Prandtl number (Pm), which measures the ratio of viscosity to resistivity. For accretion disks around black holes (BHs), Balbus & Henri (2008) had discussed the transition from large values of Pm, in the vicinity of the BH, to small values in the outer part of the disk, with Pm reaching unity for approximately 100 Schwarzschild radii (depending on several parameters, among them the mass of the BH). By invoking a thermal runaway process at the unstable interface between regions with $\mathrm{Pm} > 1$ and $\mathrm{Pm} < 1$, the authors associated this boundary with the existence of high and low X-ray states (see Remillard & McClintock 2006).

In recent years, a vivid discussion (Lesur & Longaretti 2007; Fromang et al. 2007; Käpylä & Korpi 2011; Oishi & Mac Low 2011) was devoted to the possible decline of the angular momentum transport rate with decreasing Pm, and to the intricate roles that are played here by the magnetic Reynolds number, the detailed boundary conditions, and the stratification of the disk.

Besides this relevance to the outer part of accretion disks, to protoplanetary disks (Turner & Sano 2008), and possibly even to planetary cores (Petitdemange et al. 2008), the limit of low and vanishing Pm has acquired some additional interest in connection with the recent liquid metal experiments devoted to the study of MRI (Sisan et al. 2004; Stefani et al. 2006; Nornberg et al. 2010).

While for the standard version of MRI (SMRI), characterized by only a vertical field being applied, the low Pm limit is rather smooth and unspectacular (Pessah & Chan 2008), the addition of an azimuthal field leads to dramatic effects as revealed for the first time by Hollerbach & Rüdiger (2005). The arising helical MRI (HMRI), as we call it now, was shown to work also in the limit of *vanishing* Pm since it is governed by the Reynolds and Hartmann number, quite in contrast to SMRI, which is governed by the magnetic Reynolds number and the Lundquist number. In this *inductionless limit* the induced magnetic field can be neglected with respect to the imposed one, whereas the corresponding induced currents have still to be taken into account in the Lorentz force term (see Hollerbach & Rüdiger 2005; Priede 2011).

However, as it was early shown by Liu et al. (2006), the functioning of HMRI is limited to comparably steep rotation profiles with Rossby numbers $\mathrm{Ro} < \mathrm{Ro}_{\mathrm{Liu}} = 2(1-\sqrt{2}) \approx -0.8284$ (which we henceforth will call the "Liu limit") and therefore does not extend to the astrophysically important Kepler profiles characterized by $\mathrm{Ro} = -0.75$. This essential limitation of the HMRI, together with a variety of further parameter dependencies, was confirmed in the PROMISE experiment by Stefani et al. (2006, 2007, 2009). The intricate, though continuous, transition between SMRI and HMRI, which involves a spectral exceptional point at which the inertial wave branch coalesces with the branch of the slow magnetocoriolis wave, was clarified only recently by Kirillov & Stefani (2010, 2011).

Another surprise in the limit of low Pm was, for the case of a purely or strongly dominant azimuthal magnetic field, the numerical prediction of a non-axisymmetric version of MRI, working apparently in a similar parameter region as HMRI (Hollerbach et al. 2010). Although the occurrence of MRI under the influence of a purely azimuthal magnetic field had been studied much earlier (see Hawley et al. 1995; Ogilvie & Pringle 1996; Papaloizou & Terquem 1997), the crucial effect arose again for the particular combination of low Pm and slightly steeper than Keplerian shear profiles. It has to be noticed that this azimuthal MRI (AMRI), as we call it now, works for azimuthal magnetic fields that are current-free in the considered fluid, quite in contrast to the Tayler instability (Tayler 1973; Seilmayer et al.

2012), which is a pinch-type instability in a current-carrying conducting medium.

The aim of this paper is to better understand why the scaling behavior of HMRI and AMRI, as well as their restriction to rather steep rotation profiles, is so similar. In order to clarify this point, we restrict our work completely to the short-wavelength approximation (Friedlander & Lipton-Lifschitz 2003; Hattori & Fukumoto 2003), keeping in mind that some of our conclusions will need further confirmation in more realistic simulations.

2. SHORT-WAVELENGTH ANALYSIS OF VISCOUS, RESISTIVE MRI FOR ARBITRARY AZIMUTHAL WAVENUMBERS

We start from the equations of incompressible, viscous, and resistive magnetohydrodynamics, composing the Navier–Stokes equation for the velocity field $\mathbf{u}$ and the induction equation for the magnetic field $\mathbf{B}$,

$$\frac{\partial \mathbf{u}}{\partial t} + \mathbf{u}\cdot\nabla\mathbf{u} = \frac{\mathbf{B}\cdot\nabla\mathbf{B}}{\mu_0\rho} - \frac{\nabla P}{\rho} + \nu\nabla^2\mathbf{u} \tag{1}$$

$$\frac{\partial \mathbf{B}}{\partial t} = \mathbf{B}\cdot\nabla\mathbf{u} - \mathbf{u}\cdot\nabla\mathbf{B} + \eta\nabla^2\mathbf{B}, \tag{2}$$

where $P = p + \mathbf{B}^2/2\mu_0$ is the total pressure, $\rho = \text{const}$ the density, $\nu = \text{const}$ the kinematic viscosity, $\eta = (\mu_0\sigma)^{-1}$ the magnetic diffusivity, σ the conductivity of the fluid, and μ_0 the magnetic permeability of free space. Additionally, the mass continuity equation for incompressible flows and the divergence-free condition for the magnetic induction are used:

$$\nabla\cdot\mathbf{u} = 0, \quad \nabla\cdot\mathbf{B} = 0. \tag{3}$$

In the following we consider a rotational flow in the gap between the radii R_1 and $R_2 > R_1$, with an imposed magnetic field sustained by currents external to the fluid (hence we disregard any version of the Tayler instability and its combination with MRI). Introducing the cylindrical coordinates (R, ϕ, z), we consider the stability of a magnetized Taylor–Couette (TC) flow, i.e., a steady-state background flow with the angular velocity profile $\Omega(R)$ in a (generally helical) background magnetic field,

$$\mathbf{u}_0(R) = R\,\Omega(R)\,\mathbf{e}_\phi, \quad p = p_0(R), \quad \mathbf{B}_0(R) = B_\phi^0(R)\mathbf{e}_\phi + B_z^0\mathbf{e}_z, \tag{4}$$

with the azimuthal field component

$$B_\phi^0(R) = \frac{\mu_0 I}{2\pi R}, \tag{5}$$

supposed to be produced by an axial current I, external to the fluid.

The angular velocity profile of the background TC flow is known to have the form

$$\Omega(R) = a + \frac{b}{R^2}, \tag{6}$$

where a and b are defined as

$$a = \frac{\mu_\Omega - \hat\eta^2}{1-\hat\eta^2}\Omega_1, \quad b = \frac{1-\mu_\Omega}{1-\hat\eta^2}R_1^2\Omega_1 \tag{7}$$

with the definitions

$$\hat\eta = \frac{R_1}{R_2}, \quad \mu_\Omega = \frac{\Omega_2}{\Omega_1}. \tag{8}$$

Introducing, as a measure of the steepness of the rotation profile, the Rossby number (Ro),

$$\mathrm{Ro} = \frac{R}{2\Omega}\frac{\partial\Omega}{\partial R}, \tag{9}$$

we find

$$a = \Omega(1+\mathrm{Ro}), \quad b = -\Omega R^2\mathrm{Ro}. \tag{10}$$

To study flow and magnetic field perturbations on the background of the magnetized TC flow, we linearize the Navier–Stokes and induction equation in the vicinity of the stationary solution by assuming $\mathbf{u} = \mathbf{u}_0 + \mathbf{u}'$, $p = p_0 + p'$, and $\mathbf{B} = \mathbf{B}_0 + \mathbf{B}'$ and leaving only terms of first order with respect to the primed quantities.

Then, by using a short-wavelength approximation (the details of the derivation will be published elsewhere) in the frame of the geometrical optics approach (see, e.g., Landman & Saffman 1987; Dobrokhotov & Shafarevich 1992; Friedlander & Lipton-Lifschitz 2003; Hattori & Fukumoto 2003; Lebowitz & Zweibel 2004; Mizerski & Lyra 2012), we end up with a system of four coupled equations for the perturbations of arbitrary azimuthal dependency that generalize the corresponding equations derived in Kirillov & Stefani (2010). From those four coupled equations, we can deduce the dispersion relation

$$p(\gamma) := \det(H - \gamma E) = 0, \tag{11}$$

where E is the unit matrix and the matrix H has the form

$$H = \begin{pmatrix} -im\Omega - \omega_\nu & 2\alpha^2\Omega & i\frac{m\omega_{A_\phi}+\omega_A}{\sqrt{\rho\mu_0}} & -\frac{2\omega_{A_\phi}\alpha^2}{\sqrt{\rho\mu_0}} \\ -2\Omega(1+\mathrm{Ro}) & -im\Omega-\omega_\nu & 0 & i\frac{m\omega_{A_\phi}+\omega_A}{\sqrt{\rho\mu_0}} \\ i(m\omega_{A_\phi}+\omega_A)\sqrt{\rho\mu_0} & 0 & -im\Omega-\omega_\eta & 0 \\ 2\omega_{A_\phi}\sqrt{\rho\mu_0} & i(m\omega_{A_\phi}+\omega_A)\sqrt{\rho\mu_0} & 2\Omega\mathrm{Ro} & -im\Omega-\omega_\eta \end{pmatrix}. \tag{12}$$

In Equation (12) we have used the following definitions for the viscous, resistive, and the two Alfvén frequencies corresponding to the vertical and the azimuthal magnetic field:

$$\omega_\nu = \nu|\mathbf{k}|^2 \tag{13}$$

$$\omega_\eta = \eta|\mathbf{k}|^2 \tag{14}$$

$$\omega_A^2 = \frac{k_z^2 B_z^{0\,2}}{\rho\mu_0} \tag{15}$$

$$\omega_{A_\phi}^2 = \frac{\left(B_\phi^0\right)^2}{\rho\mu_0 R^2}. \tag{16}$$

Note that $|\mathbf{k}|^2 = k_R^2 + k_z^2$ and $\alpha = k_z/|\mathbf{k}|$, where k_R, m, and k_z are the radial, azimuthal, and axial wavenumbers of the perturbation. In the absence of the magnetic fields, the dispersion relation determined by the matrix H reduces to that derived already by Krueger et al. (1966) for the non-axisymmetric perturbations of the hydrodynamical TC flow. Choosing, additionally, $m = 0$, we reproduce the result of Eckhardt & Yao (1995). In the presence of the magnetic fields and $m = 0$, we arrive at the dispersion relation derived by Kirillov & Stefani (2010).

The dispersion relation (11) generated by the matrix (12) can be rewritten completely in terms of dimensionless numbers, i.e., Rossby number (Ro), magnetic Prandtl number (Pm), ratio of the two Alfvén frequencies (β), Hartmann number (Ha), Reynolds number (Re), and a rescaled azimuthal wavenumber n:

$$\mathrm{Pm} = \frac{\nu}{\eta} = \frac{\omega_\nu}{\omega_\eta} \tag{17}$$

$$\beta = \alpha \frac{\omega_{A_\phi}}{\omega_A} \tag{18}$$

$$\mathrm{Re} = \alpha \frac{\Omega}{\omega_\nu} \tag{19}$$

$$\mathrm{Ha} = \alpha \frac{B_z^0}{k\sqrt{\mu_0 \rho \nu \eta}} \tag{20}$$

$$n = \frac{m}{\alpha}. \tag{21}$$

We stress that in this paper β must not be confused with the so-called plasma beta, i.e., the ratio of gas pressure to magnetic pressure.

After rescaling the spectral parameter as $\gamma = \lambda\sqrt{\omega_\nu \omega_\eta}$, we end up with the complex polynomial dispersion relation

$$\begin{aligned} p(\lambda) = {} & a_0\lambda^4 + (a_1 + ib_1)\lambda^3 + (a_2 + ib_2)\lambda^2 \\ & + (a_3 + ib_3)\lambda + a_4 + ib_4 = 0 \end{aligned} \tag{22}$$

with the following coefficients:

$$\begin{aligned} a_0 &= 1 \\ a_1 &= 2\left(\sqrt{\mathrm{Pm}} + \frac{1}{\sqrt{\mathrm{Pm}}}\right) \\ b_1 &= 4n\mathrm{Re}\sqrt{\mathrm{Pm}}, \\ a_2 &= 2(\beta^2\mathrm{Ha}^2 - 3\mathrm{Re}^2\mathrm{Pm})n^2 + 4\beta\mathrm{Ha}^2 n + 2(1 + (1 + 2\beta^2)\mathrm{Ha}^2) \\ &\quad + 4\mathrm{Re}^2(1 + \mathrm{Ro})\mathrm{Pm} + \frac{a_1^2}{4} \\ b_2 &= 6n\mathrm{Re}(1 + \mathrm{Pm}) \\ a_3 &= a_1(\beta^2\mathrm{Ha}^2 - 3\mathrm{Re}^2\mathrm{Pm})n^2 + 2a_1\beta\mathrm{Ha}^2 n \\ &\quad + a_1(1 + (1 + 2\beta^2)\mathrm{Ha}^2) + 8\mathrm{Re}^2(1 + \mathrm{Ro})\sqrt{\mathrm{Pm}} \\ b_3 &= 4n^3\sqrt{\mathrm{Pm}}\mathrm{Re}(\beta^2\mathrm{Ha}^2 - \mathrm{Re}^2\mathrm{Pm}) \\ &\quad + 2n\mathrm{Re}(4\mathrm{Pm}^2\mathrm{Re}^2(1 + \mathrm{Ro}) + (1 + \mathrm{Pm})^2 \\ &\quad + 2\mathrm{Pm}(1 + \mathrm{Ha}^2))/\sqrt{\mathrm{Pm}} - 8(1 - n^2)\beta\mathrm{Ha}^2\mathrm{Re}\sqrt{\mathrm{Pm}} \\ a_4 &= ((\beta^2\mathrm{Ha}^2 - \mathrm{Re}^2\mathrm{Pm})n^2 + 2\mathrm{Ha}^2\beta n + \mathrm{Ha}^2 + 2\mathrm{PmRe}^2)^2 \\ &\quad + 2(2\mathrm{Re}^2\mathrm{PmRo} + 1)((\mathrm{Ha}^2\beta^2 - \mathrm{Re}^2\mathrm{Pm})n^2 \\ &\quad + 2\mathrm{Ha}^2\beta n + \mathrm{Ha}^2) - (1 + \mathrm{Pm})^2\mathrm{Re}^2 n^2 \\ &\quad + 4\mathrm{Re}^2(1 + \mathrm{Ro}) - (\mathrm{Ha}^2 + 2\mathrm{PmRe}^2)^2 + \mathrm{Ha}^4 + 1 + 4\beta^2\mathrm{Ha}^2 \\ b_4 &= 2\mathrm{Re}(1 + \mathrm{Pm})(\beta^2\mathrm{Ha}^2 - \mathrm{Re}^2\mathrm{Pm})n^3 + 4\mathrm{ReHa}^2\beta(1 + \mathrm{Pm})n^2 \\ &\quad + 2\mathrm{Re}(2(1 + \mathrm{Ro})(2\mathrm{Re}^2\mathrm{Pm} - \beta^2\mathrm{Ha}^2(1 - \mathrm{Pm})) \\ &\quad + (1 + \mathrm{Ha}^2)(1 + \mathrm{Pm}))n - 4\beta\mathrm{Ha}^2\mathrm{Re}(2 + (1 - \mathrm{Pm})\mathrm{Ro}). \end{aligned} \tag{23}$$

Note again that this complex algebraic equation of fourth order is valid for perturbations of arbitrary azimuthal wavenumber in magnetized incompressible, viscous, resistive rotating fluids exposed to current-free axial and azimuthal magnetic fields. When $n = 0$, it reduces to the dispersion relation of HMRI derived by Kirillov & Stefani (2010).

3. INDUCTIONLESS LIMIT

Proceeding quite similarly as in Kirillov & Stefani (2010), we apply the Bilharz criterion (Bilharz 1944) to the complex polynomial (22) and derive the maximum Rossby number, at which flows are prone to MRI, as a function of the remaining dimensionless numbers. In the following, we concentrate on the inductionless limit, i.e., we take the limit $\mathrm{Pm} \to 0$.

After verifying the facts that the inductionless threshold value of Ro increases monotonically with Re, so that we can take the limit $\mathrm{Re} \to \infty$, and that in this limit the threshold value of Ro increases monotonically with Ha (see Figure 1(a)), so that we can take the limit $\mathrm{Ha} \to \infty$, we obtain the following explicit expression for this maximized (with respect to Ha and Re) critical Rossby number at the threshold of MRI in the inductionless limit:

$$\begin{aligned} &\mathrm{Ro}_{\mathrm{cr}}(\beta, n) \\ &\quad = \frac{4\beta^4 + (\beta n + 1)^4 - (2\beta^2 + (\beta n + 1)^2)\sqrt{4\beta^4 + (\beta n + 1)^4}}{2\beta^2(\beta n + 1)^2}. \end{aligned} \tag{24}$$

The maximum value of the Rossby number, $\mathrm{Ro}_{\mathrm{cr}}$, is shown as a red dot in Figure 1(a). When $n = 0$, Equation (24) reduces to the threshold of HMRI in the inductionless limit found in Kirillov & Stefani (2011). Given n and β, the critical Rossby number calculated with finite values of Re and Ha is always below the majorating value, $\mathrm{Ro}_{\mathrm{cr}}(\beta, n)$, determined by Equation (24) (see Figure 1(b)). With the increase of Ha and Re, constrained by the scaling law

$$\mathrm{Re} = 2(1 + \sqrt{2})\beta^3\mathrm{Ha}^3, \tag{25}$$

the threshold shown in Figure 1(b) tends to the majorating surface $\mathrm{Ro}_{\mathrm{cr}}(\beta, n)$ shown in Figure 2(a).

The remarkably simple dependence (24) of $\mathrm{Ro}_{\mathrm{cr}}$, only on the ratio β of azimuthal to axial field and on the rescaled azimuthal wavenumber n, relies on the appropriate choice of the dimensionless parameters, in particular on "hiding" the wavenumber ratio α in them. Assuming that we have fixed the sign of β, the functional dependence of the maximum critical Rossby number (24) on β and n has a two-saddle line structure as shown in Figure 2(a).

Now, the most important result of this paper is that both saddle lines have the same height everywhere, namely, the Liu limit $\mathrm{Ro}_{\mathrm{Liu}} = 2(1 - \sqrt{2})$, independent of the particular combination of β and n. From Equation (24) it can be proved that these saddle lines, with $\mathrm{Ro}_{\mathrm{Liu}} = 2 - 2\sqrt{2}$, are governed by the two equations

$$\begin{aligned} \beta_{\mathrm{max},1}(n) &= \frac{1}{\sqrt{2} - n}, \quad \mathrm{Ro}_{\mathrm{cr}}(\beta_{\mathrm{max},1}) = 2 - 2\sqrt{2} \\ \beta_{\mathrm{max},2}(n) &= \frac{-1}{\sqrt{2} + n}, \quad \mathrm{Ro}_{\mathrm{cr}}(\beta_{\mathrm{max},2}) = 2 - 2\sqrt{2}. \end{aligned} \tag{26}$$

In Figure 2(b) the curves $\beta_{\mathrm{max},1}(n)$ and $\beta_{\mathrm{max},2}(n)$ are shown in green and red colors, respectively. Note that according to the first of Equations (26), $n = 0$ (HMRI) corresponds to $\beta = 1/\sqrt{2}$, which, being substituted into Equation (25), yields the following scaling law for the optimum combination of Re and Ha in HMRI

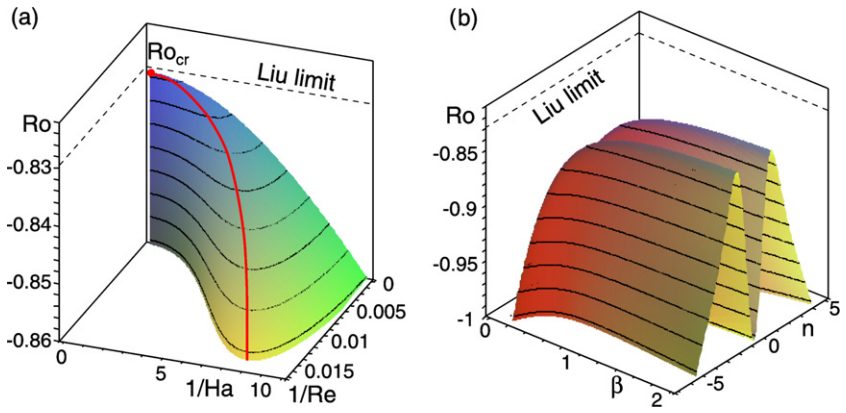

Figure 1. Inductionless limit Pm $\to$ 0: (a) At the given $n = \sqrt{2} - 1/20$ and $\beta = 20$ the threshold of MRI in the (Re^{-1}, Ha^{-1}, Ro) space with the maximum at the singular (red) point (0, 0, $\mathrm{Ro_{cr}} = 2 - 2\sqrt{2}$). The red line leading to the maximum projects into a curve approximated in the vicinity of the origin by the scaling law (25). (b) The threshold of MRI in the (β, n, Ro) space with Ha = 6 and Re determined by the scaling law (25) reaches its upper bound at $\beta \to \infty$ (AMRI), which is still below the Liu limit $\mathrm{Ro_{Liu}} = 2 - 2\sqrt{2}$.

(A color version of this figure is available in the online journal.)

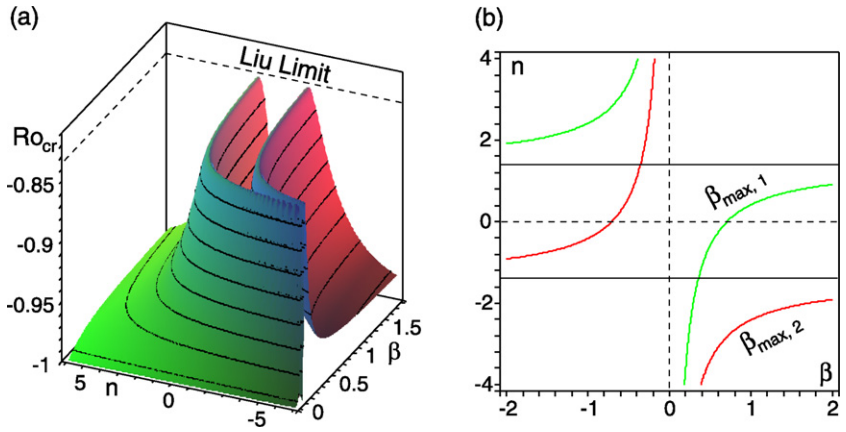

Figure 2. (a) The critical Rossby number maximized with respect to Ha and Re, given by Equation (24), in dependence on β and n. (b) The lines $\beta_{\mathrm{max},1}$ (green) and $\beta_{\mathrm{max},2}$ (red) at which the function $\mathrm{Ro_{cr}}(\beta, n)$ attains its maximal value $\mathrm{Ro_{Liu}} = 2 - 2\sqrt{2}$.

(A color version of this figure is available in the online journal.)

(Kirillov & Stefani 2010):

$$\mathrm{Re} = \frac{2+\sqrt{2}}{2}\mathrm{Ha}^3. \tag{27}$$

Therefore, even in the case of non-axisymmetric perturbations, the maximum possible value of the Rossby number prone to the MRI caused by the helical magnetic field in the inductionless limit is still $\mathrm{Ro_{Liu}} = 2 - 2\sqrt{2}$, exactly as in the case of HMRI, which is an instability with respect to the axisymmetric perturbations ($n = 0$). The relations (26) between β and n that correspond to the Liu limit give a sort of the *resonance conditions* between the components of the wavevector of the three-dimensional perturbation and the components of the helical magnetic field.

On the basis of Equations (26) connecting β and the rescaled azimuthal wavenumber n, we can ask now for the structure of the solution in terms of the original, "physical" azimuthal wavenumber m. From the definition $\alpha = k_z/|\mathbf{k}|$ we see immediately that α can take on only values between -1 and $+1$. The solution structure can thus be visualized as in Figure 3. For example, from the first of Equations (26) we see that for large values of β (AMRI), the only possible integer solution is the $m = 1$ mode, whose corresponding wavenumber ratio

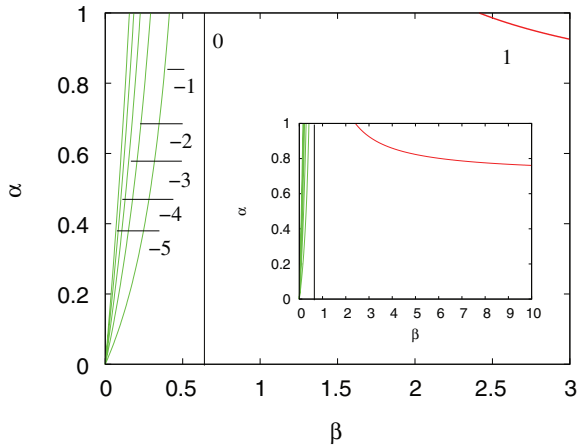

Figure 3. Range of α for the different m modes, in dependence on β.

(A color version of this figure is available in the online journal.)

converges to $\alpha = 1/\sqrt{2}$ (see also Figure 2(b)). There is a lower limit of $\beta = 1 + \sqrt{2} \approx 2.41$ for this $m = 1$ mode. Lowering β further, we find next the $m = 0$ mode (HMRI) to dominate at the Liu limit, restricted only to $\beta = 1/\sqrt{2}$ (Kirillov

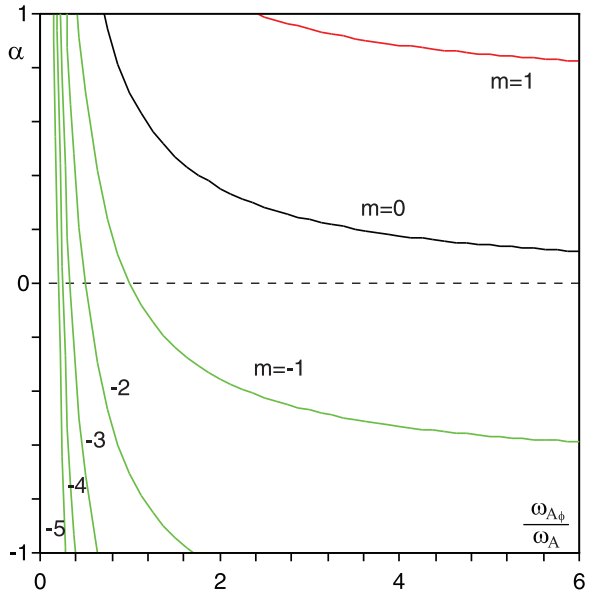

Figure 4. Range of α for the different m modes, in dependence on β/α: $m = 1$ (red line), $m = 0$ (black line), $m = -1, -2, -3, -4, -5$ (green lines).
(A color version of this figure is available in the online journal.)

& Stefani 2010). Interestingly, decreasing $\beta > 0$ even further to zero, we find a sequence of higher azimuthal modes with the sign of m that is opposite to the sign of β that maximize the critical Rossby number, illustrating the resonance phenomenon mentioned above.

Since α enters also the definition of β, it might be instructive to illustrate the mode structure also in dependence on $\beta/\alpha = \omega_{A_\phi}/\omega_A$. From Equations (26) we derive

$$\alpha = \pm\frac{\sqrt{2}}{2}\left(m + \frac{\omega_A}{\omega_{A_\phi}}\right), \tag{28}$$

where the positive sign corresponds to the first of Equations (26) and the negative sign to the second one. This means that with a given azimuthal wavenumber m, two axial wavenumbers, k_z, are associated following from Equation (28) that differ by sign only. Such combinations of wavenumbers are the most destabilizing in the sense that the magnetized TC flow is unstable at the highest possible Rossby number.

In Figure 4 we plot the positive branch of Equation (28) because the negative one is simply its reflection about the horizontal coordinate axis. We see now that the HMRI mode ($m = 0$) starts at $\omega_{A_\phi}/\omega_A = 1/\sqrt{2}$ and remains for arbitrary large values of β/α, although with an ever-decreasing wavenumber ratio, which would correspond to ever-increasing wavelengths in the z-direction. Again it is only the AMRI modes ($m = \pm 1$) that, for large β/α, maintain a physically sensible wavenumber $\alpha = \pm 1/\sqrt{2}$. The higher modes with $m \leqslant -2$ are obtained for smaller values of β/α.

Hence, when the azimuthal magnetic field is directed along the basic flow that rotates counterclockwise with respect to the z-axis, among the modes that are MRI-unstable at the Liu limit there are only two (AMRI) that corotate with the flow ($m = 1$) and simultaneously propagate along either the positive or negative z-direction. These modes are dominant when $\omega_{A_\phi}/\omega_A > 1 + \sqrt{2}$ (see the red curve in Figure 4). At moderate ratios ω_{A_ϕ}/ω_A, the Liu limit is at the axisymmetric HMRI mode. When $\omega_{A_\phi}/\omega_A \to 0$, infinitely many modes with $m \leqslant -1$ that propagate in either the negative or positive z-direction and counter-rotate with respect to the basic flow can cause instability at the Liu limit. Note, however, that at finite Re and Ha the highest modes will be inhibited (see Figure 1(b)).

4. CONCLUSION

Using a short-wavelength approach, we have presented a unifying picture of the inductionless forms of MRI. We have identified a continuous function of the maximum critical Rossby number that incorporates both types of instability. We were lead to the conclusion that in the limit of small ratios of azimuthal to axial field there should be inductionless MRI versions with higher m modes, counter-rotating with respect to the basic flow, although this needs further confirmation at least by a one-dimensional linear stability analysis. Most interestingly, the Liu limit has turned out to be of quite universal significance, since the range of its validity has been extended from the realm of axisymmetric HMRI to that of non-axisymmetric MRI versions. Actually, soon after its derivation in the WKB approximation, the relevance of the Liu limit had been questioned by Rüdiger & Hollerbach (2007), who had found an apparent extension of this limit in global simulations when at least one of the radial boundary conditions was assumed to be electrically conducting. Later, though, utilizing another definition of the notion "quasi-Keplerian" for TC flows, the Liu limit was rehabilitated by Priede (2011).

Going beyond the inductionless limit, for small but finite Pm Kirillov & Stefani (2011) had shown that the Liu limit can be slightly extended to a new limiting value Ro ≈ -0.802, which is, however, still below the Kepler value. To bridge the remaining gap between HMRI/AMRI at small Pm and the corresponding versions of MRI at larger Pm (including 1) is a more intricate task, though. It had been shown by Kirillov & Stefani (2010) that the transition between standard MRI and HMRI involves a spectral exceptional point at which the branches of the inertial wave and the slow magneto-Coriolis wave coalesce. It is this exceptional point that resolves the apparent paradox that the transition between the two versions is continuous (Hollerbach & Rüdiger 2005) despite the fact that HMRI can be characterized as a weakly destabilized inertial wave (Liu et al. 2006), while standard MRI is known to be a destabilized slow magneto-Coriolis wave. We believe that, with varying Pm, quite similar transitions will also occur for AMRI (and the higher m-modes discussed in this paper), although we have to leave the detailed investigation for further work.

As a side remark, the determination of such limits is even more complicated by the necessity to distinguish, for traveling waves as in HMRI, between convective and absolute (or global) instabilities, which has been thoroughly discussed by Priede & Gerbeth (2009) and was shown to be experimentally important by Stefani et al. (2009).

From the strictly astrophysical point of view, our support for the Liu limit may appear disappointing, since it would exclude any relevance of the inductionless versions of MRI to accretion disks with Keplerian rotation. A subtle question in this respect is, however, connected with the saturation mechanism of the MRI that could, possibly, lead to modified shear profiles. With the main focus on low Pm flows, Umurhan (2010) considered the possibility that the saturation of MRI could lead to modified flow structures within parts of steeper shear, sandwiched with parts of shallower shear. Moreover, for protoplanetary disks (characterized by low Pm) the simulations of Kato et al. (2009) had also shown the appearance of layers with increased shear.

By virtue of a possible sudden onset within such segments of steepening shear, the low Pm and inductionless MRI versions could thus play a certain role in real astrophysical settings.

This work was supported by the Deutsche Forschungsgemeinschaft in frame of SFB 609 and SPP1488. O.N.K. gratefully acknowledges the support of the Japan Society for the Promotion of Science and of the Alexander von Humboldt Foundation. We thank Rainer Hollerbach and Günther Rüdiger for numerous discussions on the various versions of MRI.

REFERENCES

Balbus, S. A., & Hawley, J. F. 1991, ApJ, 376, 214
Balbus, S. A., & Henri, P. 2008, ApJ, 674, 408
Bilharz, H. 1944, Z. Angew. Math. Mech., 24, 77
Dobrokhotov, S., & Shafarevich, A. 1992, Math. Notes, 51, 47
Eckhardt, B., & Yao, D. 1995, Chaos Solitons Fractals, 5, 2073
Friedlander, S., & Lipton-Lifschitz, A. 2003, Localized Instabilities in Fluids. Handbook of Mathematical Fluid Dynamics, Vol. II, ed. S. J. Friedlander & D. Serre Elsevier (Amsterdam: North-Holland), 289
Fromang, S., Papaloizou, J., Lesur, G., & Heinemann, T. 2007, A&A, 476, 1123
Hattori, Y., & Fukumoto, Y. 2003, Phys. Fluids, 15, 3151
Hawley, J. F., Gammie, C. F., & Balbus, S. A. 1995, ApJ, 440, 742
Hollerbach, R., & Rüdiger, G. 2005, Phys. Rev. Lett., 95, 124501
Hollerbach, R., Teeluck, V., & Rüdiger, G. 2010, Phys. Rev. Lett., 104, 044502
Käpylä, P. J., & Korpi, M. J. 2011, MNRAS, 413, 901
Kato, M. T., Nakamura, K., Tandokoro, R., Fujimoto, M., & Ida, S. 2009, ApJ, 691, 1697
Kirillov, O. N., & Stefani, F. 2010, ApJ, 712, 52
Kirillov, O. N., & Stefani, F. 2011, Phys. Rev. E, 84, 036304
Krueger, E. R., Gross, A., & Di Prima, R. C. 1966, J. Fluid Mech., 24, 521
Landman, M. J., & Saffman, P. G. 1987, Phys. Fluids, 30, 2339
Lebowitz, N. R., & Zweibel, E. 2004, ApJ, 609, 301
Lesur, G., & Longaretti, P.-Y. 2007, MNRAS, 378, 1471
Liu, W., Goodman, J., Herron, I., & Ji, H. T. 2006, Phys. Rev. E, 74, 056302
Mizerski, K. A., & Lyra, W. 2012, J. Fluid. Mech., 698, 358
Nornberg, M. D., Ji, H., Schartman, E., Roach, E., & Goodman, J. 2010, Phys. Rev. Lett., 104, 074501
Ogilvie, G. I., & Pringle, J. E. 1996, MNRAS, 279, 151
Oishi, J. S., & Mac Low, M.-M. 2011, ApJ, 740, 18
Papaloizou, J. C. B., & Terquem, C. 1997, MNRAS, 287, 771
Pessah, M. E., & Chan, C. 2008, ApJ, 684, 498
Petitdemange, L., Dormy, E., & Balbus, S. A. 2008, Geophys. Res. Lett., 35, 15305
Priede, J. 2011, Phys. Rev. E, 84, 066314
Priede, J., & Gerbeth, G. 2009, Phys. Rev. E, 79, 046310
Remillard, R. A., & McClintock, J. E. 2006, ARA&A, 44, 49
Rüdiger, G., & Hollerbach, R. 2007, Phys. Rev. E, 76, 068301
Seilmayer, M., Stefani, F., Gundrum, T., et al. 2012, Phys. Rev. Lett., 108, 244501
Sisan, D. R., Mujica, N., Tillotson, W. A., et al. 2004, Phys. Rev. Lett., 93, 114502
Stefani, F., Gerbeth, G., Gundrum, T., et al. 2009, Phys. Rev. E., 80, 066303
Stefani, F., Gundrum, T., Gerbeth, G., et al. 2006, Phys. Rev. Lett., 97, 184502
Stefani, F., Gundrum, T., Gerbeth, G., et al. 2007, New J. Phys., 9, 295
Tayler, R. J. 1973, MNRAS, 161, 365
Turner, N. J., & Sano, T. 2008, ApJ, 679, L131
Umurhan, O. M. 2010, A&A, 513, A47